Modern Physics Letters A
Vol. 30, No. 17 (2015) 1540023 (14 pages)

DOI: 10.1142/S0217732315400234

Dose monitoring in particle therapy

Riccardo Faccini
Dipartimento di Fisica, Università di Roma "La Sapienza" and
INFN Sezione di Roma, P.le A. Moro 2, 00185 Rome, Italy
riccado.faccini@roma1.infn.it

Vincenzo Patera
Dipartimento di Scienze di Base e Applicate per l'Ingegneria,
Università di Roma "La Sapienza", Via A. Scarpa 16, 00161 Rome, Italy
and
INFN Sezione di Roma, P.le A. Moro 2, 00185 Rome, Italy

Received 14 January 2015
Accepted 16 February 2015
Published

Ion therapy is an emerging technique used for the treatment of solid cancers. The monitoring of the dose delivered during such treatments and the on-line knowledge of the Bragg Peak (BP) position is still a matter of research. This paper reviews the current understanding of which radiation is produced during the interaction of the beam with the patient, the corresponding techniques developed to detect it and the level of understanding of the conversion between the emission spectra and the dose profile. It also performs a comparison between the different approaches.

Keywords: Particle therapy; dosimetry.

1. Introduction

The use of ion beams has become more and more widespread as an effective therapy for the treatment of solid cancers (Particle Therapy, PT). These beams have a characteristic energy release localized close to the end of their range (the Bragg Peak, BP). The most common beams used in PT are protons, mainly due to cost and space motivations. Carbon ions are another very effective choice, but in future also the use of ^{4}He and ^{16}O beams is envisaged. Due to their very favorable profile of released dose in tissue, the beams of light ions can be very effective in destroying the tumor and sparing the adjacent healthy tissue in comparison to the standard X-ray-based treatment. On the other hand, the higher spatial selectivity of PT asks for a dedicated approach to the delivered dose monitoring.

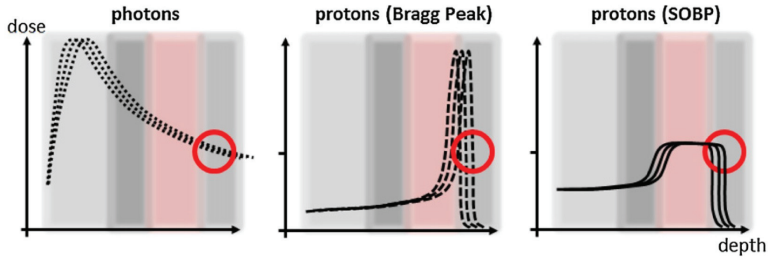

Fig. 1. (color online) Effect of the beam range uncertainty, from left to right, in conventional radiotherapy, with mono-energetic proton beam, with a clinical particle therapy beam setup (SOBP).[1] The pink region represents the tumor, the lightest gray on the left soft tissue, the two other gray regions organs at risk.

The uncertainty on the position of the dose release in PT treatments can be due to different factors, such as quality and calibration of the Computed Tomography (CT) images or possible morphologic changes occurring between CT and each of the several irradiation sessions, operated in different days, that compose a PT treatment. Finally also patient mis-positioning and organ motion during the treatment itself can be sources of uncertainty. All these effects can add up to give an overall uncertainty of the order of few millimeters[1] (see also Fig. 1).

To take into account the uncertainty of the dose release distribution, the software that provides the treatment setting to the beam accelerator (the Treatment Planning System, TPS) is forced to account for a safety margin of the same size around the tumor and the organ at risk. Furthermore the number and the geometry of the beams fields of the treatment are usually chosen to minimize the risk for the patient due to possible undetected dose release misplacement.

A procedure to monitor the dose release, better if provided in real time, can increase the quality assurance of a PT treatment.

Standard techniques, such as the ionization chamber, can be used to check the transverse position and shape of the beam. Unfortunately no information can be retrieved about the longitudinal dose pattern as in conventional radiotherapy with photons because the hadron beam is completely absorbed inside the patient. The main issue of the PT dose monitoring is then the measurement of the longitudinal shape of the dose release, and namely of the position of the BP of the beam.

To this aim new approaches must be developed, taking into account that the energy release of the beam is largely driven by the electromagnetic interactions with the patient, while strong interactions are needed to produce radiation that can escape the patient and allow for an imaging of its source. Three are the nuclear processes that can yield a radiation suited for this purpose: production of β^+ emitters nuclei, excitation of nuclei and fragmentation.

Nuclear β^+ decays produce positrons that can be traced exploiting their annihilation with electrons that yield back-to-back 511 keV photon pairs (PET photons). As tissue is mostly constituted of carbon, hydrogen and oxygen, the most likely

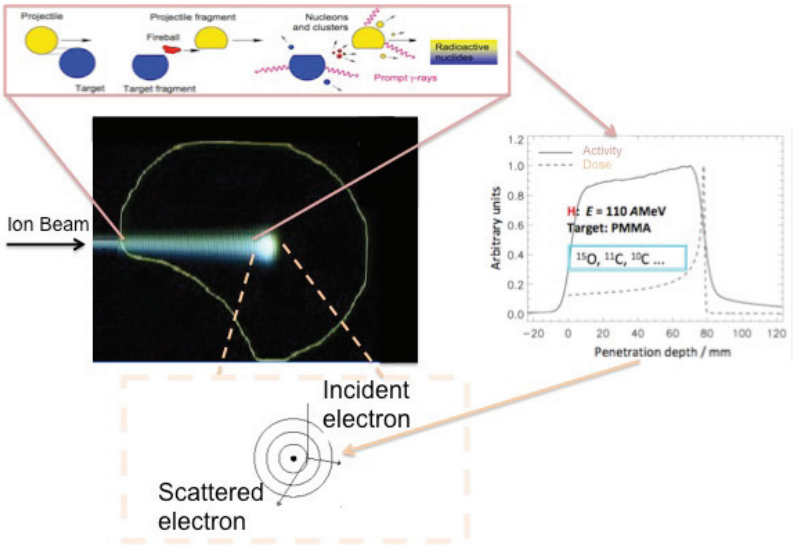

Fig. 2. Scheme of the dose profiling procedure: while the energy release happens mostly by ionization (bottom box), the dosimetry requires strong interactions between beam ions ("Projectile" in the top box) and the patient tissues ("Target"). The conversion between the activity profile and the dose profile is deputed to a Monte Carlo (MC) simulation (right box).

β^+ emitting isotopes that can be formed are ^{10}C (with lifetime $\tau = 28$ s), ^{11}C ($\tau = 29$ min), ^{14}O ($\tau = 102$ s), ^{15}O ($\tau = 176$ s), ^{13}N ($\tau = 14$ min). The relative composition depends on the projectile.

The passage of the beam in the patient can also excite nuclei whose de-excitation produce photons. Since this process is mediated by strong interactions, it has very short (< 1 ns) decay times and the produced photons, that can be used for monitoring, are prompt. Albeit dominated by the 4.44 MeV and 6.13 MeV lines from C^* and O^* respectively, there is a large continuum spectrum up to almost 10 MeV.

Finally, the production of charged fragments is a high cross-section strong process where either the projectile and the target nucleus or both fragments into charged ions of smaller mass. The understanding of this process is particularly difficult because the energy regime of interest, projectiles that at the moment of the interaction range between 20 MeV/u and 200 MeV/u, is relatively low and therefore the strong interactions are particularly difficult to model. During the last decade several measurements have been performed to evaluate the dose contribution to healthy tissues due to the beam production of these fragment, but little or no attention has been paid to the production of large angle, low ionizing, high penetrating proton component, that can be exploited for monitoring purposes.

The detection of these secondary particles is the basic requirement for monitoring the dose distribution, but another crucial step is the correlation between the detected spatial distribution of strong interactions of the beam with the patient and the released dose profile (see Fig. 2). This task is very demanding due to the

required knowledge in the patient's heterogeneous media of both the electromagnetic interactions (that provide the dose) and the strong interactions (that yield the monitoring signal).

It must be remarked that the necessary unfolding procedure should not use the water equivalent approximation, commonly used by TPS, and which takes only into account the electron density of the patient. While it is enough to model the dose release, it does not allow for a correct estimate of the signal produced by strong interactions, which depend also on the nuclear composition of the patient tissue.

A viable approach to predict the emission pattern of the secondary radiation produced by the beam for a given patient is the use of MC codes. The most commonly used codes are FLUKA[2] and GEANT.[3] These packages were designed for high energy physics experiments, but their application to medicine is increasing. The level of agreement between the prediction of these codes and the secondary flux data is not yet optimal but is rapidly improving thanks to the ongoing research described here.

The proposed methods for dose profiling can be grouped by the type of nuclear process that they exploit. Furthermore, the techniques exploiting the β^+ decay, due to its long lifetime, can be separated between "*in-situ*" and "in-beam" depending on whether the imaging is performed after or during the treatment.

This paper will discuss the techniques currently under development (Secs. 2–4) with particular attention to the studies of the energy and angular spectra of the out-coming particles. Finally we will compare the expected sensitivities of the different approaches (Sec. 5).

2. Monitoring with PET Photons

Among the processes that occur during a PT treatment, β^+ decays are the easiest to detect, in particular in a medical environment that already exploits instrumentation for PET scans. Therefore, the idea to measure the β^+ activity after irradiation with protons to estimate the dose profile dates back to 1978.[4]

The correlation between the distribution of β^+ emitters and the BP is evident in the case of carbon (see Fig. 3) and the comparison between the observations with MC simulation is sufficient for a first clinical evaluation. More complicated is the case of beams of lighter ions because, as shown in Fig. 3 for protons, β^+ emitters are produced along the whole path before the BP. This implies that the core of the information on the BP position comes from the distal emitters, that are a small fraction.[5] On the positive side, it was observed that the lower the mass of the incident ion, the larger the production rate: ^{7}Li and proton beams yield respectively 1.8 and 3 times more positrons than ^{12}C.[6,7]

Another complication in this approach is the fact that the lifetimes of the emitting nuclides are comparable with the duration of the treatments and that several nuclides with different life-times contribute to the signal.[8] This implies that in each moment the observed rates are the sum of several contributions since in each treat-

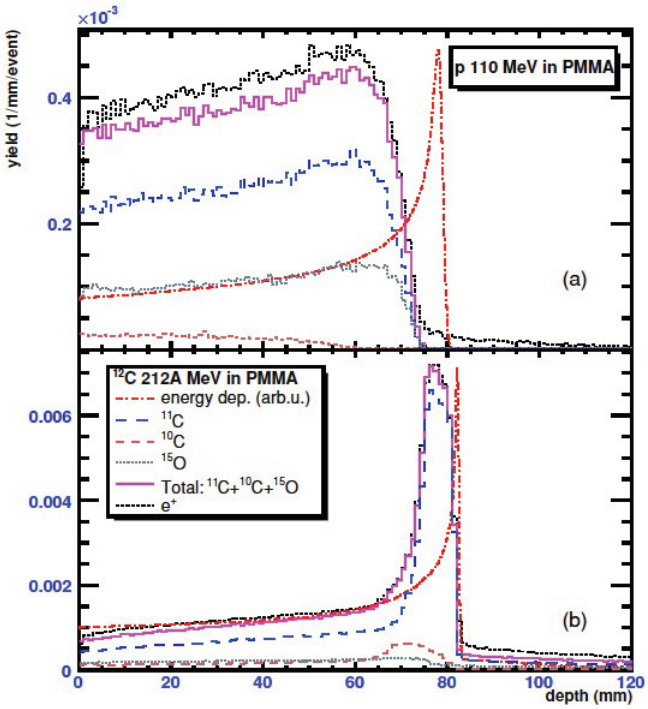

Fig. 3. Comparison between the distributions of β^+ emitters with the dose profile in the case of proton (top) and carbon (bottom) beams (predictions with the GEANT MC code in Ref. 10).

ment the pencil-beams scan the volume. Therefore, an *ad hoc* mathematical filtering is required to unfold the dose profile.[9]

The intrinsic limitation of this technique is given by the reduced activity produced by the beam with respect to a standard PET activity (up to two orders of magnitude less) and to the long lifetimes of the β^+ emitters (up to 20 mins.) with respect to the irradiation time. The PET integration time is limited by the metabolic wash-out and to the patient workflow. Different procedures have been attempted taking PET data after the irradiation, either in the treatment room (in-root PET) or moving the patient to a standard PET scanner (off-line PET). Finally PET monitoring procedures during irradiation are under development. Figure 4 shows the different timings of these three approaches.

The off-line approach has been extensively tested,[11,12] and the intrinsic alignment uncertainties have been reduced with an accurate positioning. However the time needed to move the patient to a standard PET scanner enhances the metabolic wash-out effect on the accuracy. A workflow that relies heavily on MC simulation including bio-kinetic information[13] to unfold the dose profile (see Fig. 5) is needed to deal with such an effect.

A more favorable in-room setup has been tested[14,15] where the patient is monitored after the irradiation for several minutes in the same treatment position. A

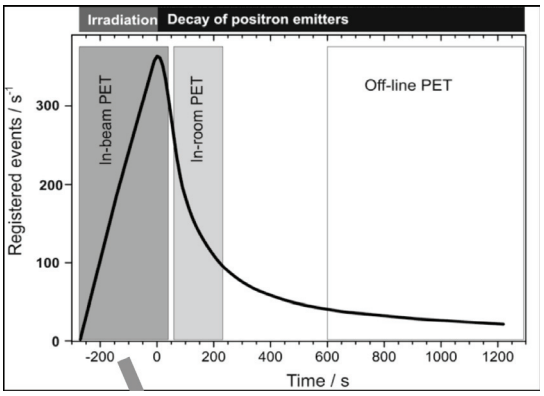

Fig. 4. Comparison of the data taking times for in-beam, in-room and off-line PET monitoring.

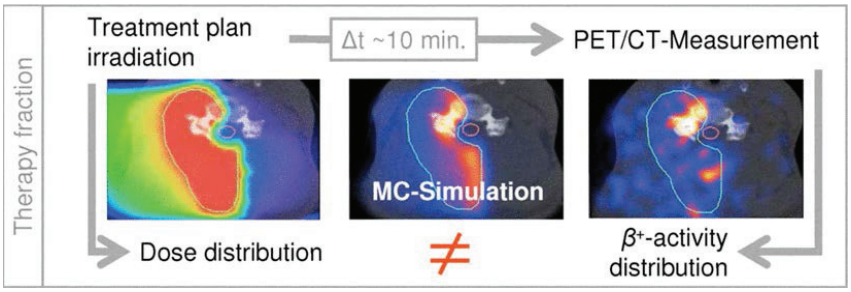

Fig. 5. (color online) Treatment fraction with post-therapeutical PET scan: the planned therapy irradiation leads to a dose distribution in the target volume (green structure), that is not directly measurable in the patient (left panel). After the subsequent patient transfer to the PET/CT scanner, the activated tissue can be imaged with a PET scan (right panel). Since dose and activity distributions are different quantities, MC methods are used to close the gap (middle panel).[20]

range control accuracy of few mm and a satisfactory control of the daily inter-session anatomical changes have been obtained. In spite of that, the impact of this procedure (both for data taking and analysis) on the patient workflow put some limitation on the use in the clinical practice.

To overcome these limitations a system to measure the β^+ emissions during the irradiation was developed at GSI on ^{12}C beams.[16,17] Albeit exploiting PET scanners that are designed to operate in a much cleaner environment, the results on more than 400 patients were encouraging. This technique needs a limited size detector setup to be integrated with the beam nozzle and the patient couch. On the other hand, the patient is in the same position of the treatment during data taking, short lived emitters can contribute to the signal and there is very limited impact on the patient workflow. In spite of the reduced angular acceptance, enough sensitivity can be achieved on beam range and beam lateral profile.[18,19]

The need for an articulated unfolding procedure asks for a sensitivity that is hard to reach with the statistics available during the treatment. Because a limiting

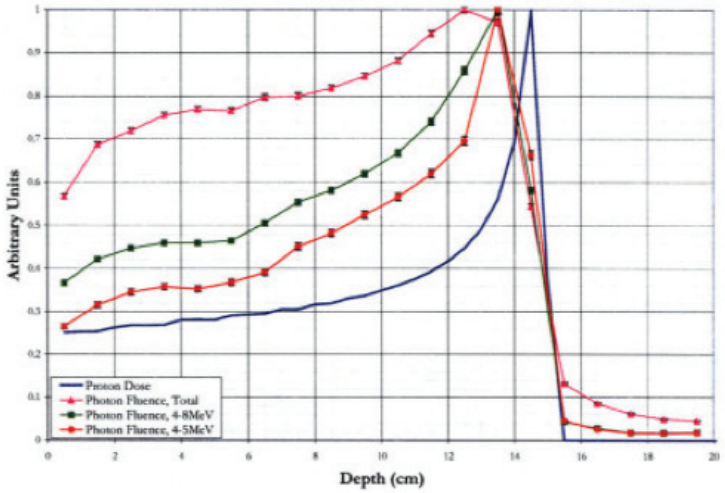

Fig. 6. Relationship between PG source distribution and dose profile in case of proton beams.[24]

factor is the presence of large background of neutral particles induced by the beam,[19] optimized detectors are under development. Particular importance is given to the optimization of the crystals and readout to minimize the time and spatial resolution.[8,21,22] These studies lead to a first in-beam test with a two heads prototype[23] which showed that the inclusion of data acquired during the irradiation improves both the precision and the accuracy of the range measurement with respect to data acquired only after irradiation.

3. Monitoring with Prompt Photons

Due to the limitations of the PET approach, other complementary techniques were explored. Among the possible strong processes described above, nuclear de-excitation is already used in SPECT and it is characterized by half-lives negligible with respect to the time lapses involved in a treatment. Therefore, dose profiling based on nuclear de-excitation gamma emission (Prompt Gammas, PG) is a good candidate to complement the PET photons.

Two are the aspects that have been investigated: the characteristics of the emitted radiation (PG rates and energy spectra for different ion types, directions and energies) and the development of appropriate detectors. It became indeed immediately clear that the energies of the emitted photons are higher than the SPECT ones and therefore the conventional detectors do not serve the purpose.

The initial studies were focused on proton beams[26–28] and they showed a correlation between the distal fall-off of the BP and the PG emission profile. At the BP the emission is depressed (see Fig. 6) but there is an enhancement in the PG rate approximately 1 cm before the BP. The energy spectrum of the out-going radiation was simulated and studied with HPGe detectors.[29,30] As shown in Fig. 8, the

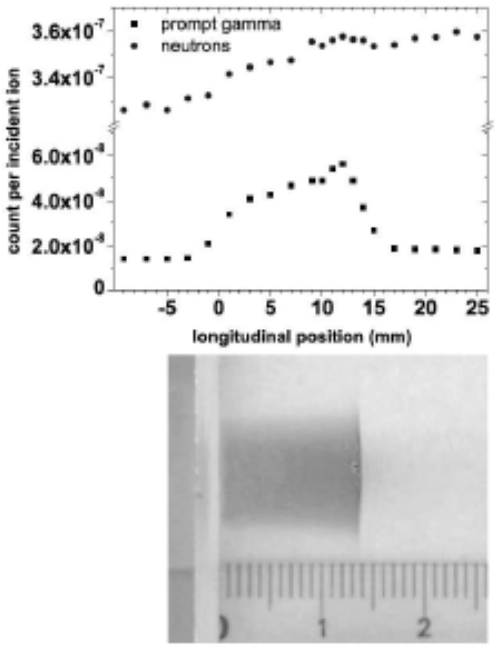

Fig. 7. Relationship between PG and neutron source distribution and dose profile in case of carbon-ion (bottom) beams.[33] The bottom image shows the location of the BP directly on the PMMA target after irradiation.

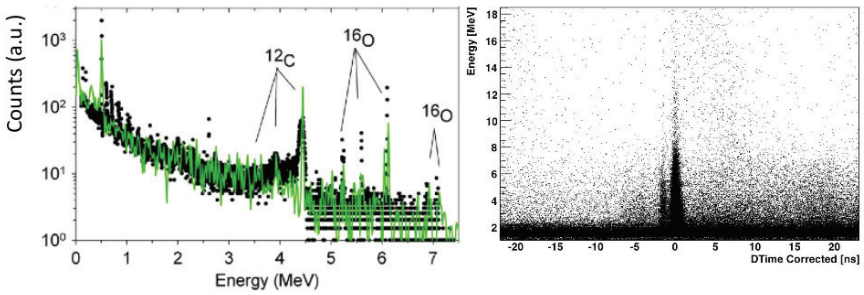

Fig. 8. Left: energy spectrum of PGs emitted from the irradiation of protons on a lucite target[29] in data (dots) and MC (line). Right: correlation between PG energy and time of flight (TOF) in the interaction of carbon ions on PMMA.[34]

spectrum presents a continuum component, ranging up to about 8 MeV and decreasing with energy, and two dominant lines from $^{12}C^*$ and $^{16}O^*$ at 4.44 MeV and 6.13 MeV, respectively. Such lines were shown to have different intensities depending on the traversed tissue, thus allowing for the determination of its composition, in particular the oxygen concentration.[31]

As far as the carbon beams are concerned (see Fig. 7), the PG emitters are distributed in the region before the BP with no significant enhancement.[25,32,33]

The PG energy spectra are dominated by the carbon line (4.44 MeV) due to its presence both in the beam and in the target.[34,35]

As far as the rates are concerned, all measurements report counts on the detectors consistent with having a statistical error comparable with the uncertainty on the BP due to MC simulation even with a therapeutical rate of 2 Gy/min ($\approx 10^9$ particles/min). In this respect, the most accurate measurement[34] reports an observed rate in the case of a carbon-ion beam with $E = 80$ MeV/u of $(3.04 \pm 0.20) \times 10^{-6}$ counts with a photon energy $E_\gamma > 2$ MeV at 90° with respect to the beam, per impinging carbon. Correcting for efficiency and acceptance, the production rate was estimated to be $dN_\gamma/dN_C/d\Omega(E_\gamma > 2 \text{ MeV}, 90°) = (2.32 \pm 0.15) \times 10^{-3}$ sr^{-1}. In addition to evaluating the rates, it is important to compare the observed yields with the expectations from MC, above all since discrepancies are an indication of ill-reproduced processes in the simulation that is used to estimate the dose profile from the observed spectra. All direct comparisons[25,34,35] resulted in an excess of PG production in MC, the smallest effect (40%) being in the case of FLUKA.[35]

The potentiality of the technique is mostly related to the correlation of the PG emission distribution fall-off with the BP position. However the accuracy on this correlation depends significantly on the detector choice and the standard SPECT detectors are not suitable due to the high energy of the PG that rules out the SPECT collimator system designed for the 140 keV photon from ^{99m}Tc. Thus, new devices must be designed for the detection of photon flux with the bulk of the energy spectrum in the 1–8 MeV range, arriving within a fraction of ns from the parent particle of the beam. The main background to this signature is represented by the other products of the nuclear interactions between the beam and the patients, mostly neutrons and delayed photons induced by the neutrons interaction with the environment. The background features depend on surrounding materials, the irradiation field features and the patient morphology itself.

The first studies[26–28] made use of a gamma camera with a collimator to determine the direction of the incoming photon and a borated shielding against neutrons.

There have been several attempts to optimize the geometry, in particular using slit cameras[36] and knife-edge-shaped collimators.[37] An accuracy of the order of 1 mm on a single proton pencil beam is reported[36] coupling a knife-edge slit camera with LYSO crystal scintillators read-out by SiPM.

Slow neutrons could be discriminated because of the longer time that they take to reach the detector, i.e. by measuring the TOF between the arrival of the projectile ion and the measurement in the photon detector. To this aim, NaI detectors with time measurements were used in Refs. 25, 32 and 33, but the best performances were obtained by exploiting the ≈ 300 ps time resolution of a LYSO detector,[34] as shown in Fig. 8 where the signal is clearly separated from the background. However a TOF based discrimination is not straightforward to be applied in clinical practice, due to the high ion delivery rates and the nontrivial time structure of therapeutic beams.[19]

This mechanical collimation approach strongly reduces the acceptance of the detector and therefore several alternatives were explored. The acceptance and the background suppression are strongly aided by the use of Compton cameras: neutrons do not release energy in the scatterer and there is no need for a passive collimator. This advantage is almost compensated by the reduced reconstruction efficiency due to the need of simultaneous detection of the photon and electron in Compton event to reconstruct the PG emission point. In spite of that, the three-stage Compton camera optimized in Refs. 38–40 reached a statistics of $\approx 10^{-5}$ PGs per impinging proton.

4. Monitoring with Charged Particles

Both described approaches rely on photon detection, which asks for collimation, mechanical or electronic, to estimate the origin of the photon itself. Much easier would be such determination if charged particles were exploited and a tracking device was used to measure their trajectories.

In case ions heavier than hydrogen are used, effects deriving from the fragmentation of the impinging nuclei become more and more evident with increasing ion mass. Since the fragmentation products are charged and have lower charge and a velocity close or even larger to that of the primary ions, they have a lower stopping power. This results in a longer range of the fragments in comparison to the primary particles, leading to a characteristic dose tail behind the BP. This effect is clinically very relevant and it has been studied with devoted nuclear cross-section experiments[43,44] and with measurements of fluxes in carbon ion collisions with water.[41,45–48] These tests showed that fragmentation products are peaked in the forward region and mostly contained within few degrees of the beam axis, a part from protons, that represent the largest sample and show tails at large emission angles and energies (see Fig. 9).

Recent studies showed that this effect can also be exploited to estimate the distal edge of the dose profile since there is a correlation between the distribution of the fragmentation vertex and the BP (see Fig. 9) and the quality of the reconstruction of the trajectory of the single charged particle compensates for reductions in statistics. Low angle measurements[42,49] showed that in principle, using solid state tracking devices at 30° with respect to the beam direction, the distal edge of the beam could be estimated with an accuracy of 1.3 mm. In addition, variations in the beam width could be measured with a precision of 0.9 mm.

A large acceptance detector that reconstructs the secondary charged particles direction can be even placed at large angle with respect to the beam axis, where for geometrical reasons the sensitivity to the origin of the fragment is optimal[50] and is independent from the beam spot size. The measurements performed under these conditions revealed that together with protons also a significant fraction of deuterons and tritia was produced. They also quantified the decrease in statistics with increasing angle (see Fig. 10). In the same experiments, the distribution of

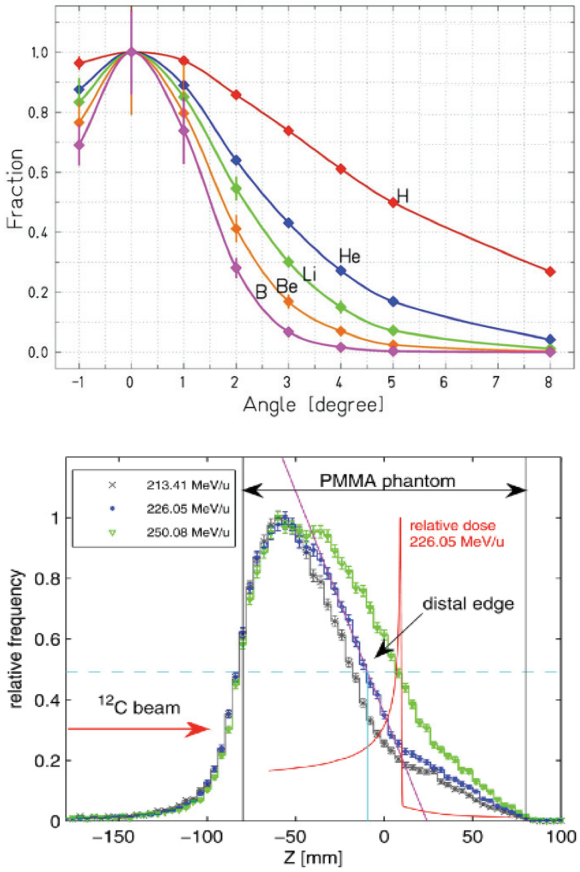

Fig. 9. Top: angular distribution of the fragmentation products with respect to the beam axis.[41] Bottom: comparison between the charged tracks distribution in the target and the dose profile.[42]

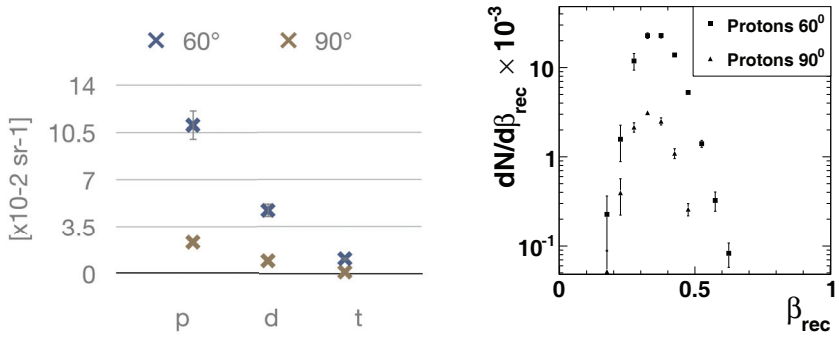

Fig. 10. Left: measured production rates of protons, deuterons and tritia at 60° and 90° from the beam axis. Right: distribution of the β of the produced protons.[50]

the β of the particles was measured, revealing that the proton end-point is at $\approx$350 (140) MeV at 60° (90°). The optimal measurement angle seems to be at 60° with the beam axis, where 3 mm resolution could be achieved for each therapeutic pencil beam of the treatment.

5. Conclusions and Outlook

Nowadays, none of the techniques described in this paper is adopted yet in clinical practice, but possible solutions seem achievable, at least for the task of beam range monitoring. More complex techniques are needed to quantitatively measure the dose release to the patient.

The baseline approach, the only one already tested on patients, is PET. A straightforward application of standard PET machine has drawbacks as reduced sensitivity with respect to standard imaging and not easy integration in the standard patient workflow. Even with these caveats, a satisfactory control on the treatment quality after the irradiation has been achieved with in-room and off-line technique, but several research groups are trying to optimize a in-beam dedicated device.

Techniques using prompt secondaries are appealing because in principle allow for an immediate feedback to the machine in case of mismatch between the measured and expected dose profile. As reported in the previous sections, statistics is the main limitation both for PG than for charged secondary, and to overcome this situation a sizable research and development effort is ongoing that borrow technology from nuclear and particle physics. The PG approach is now starting to give the first working prototype, focused mainly on proton beams. The test on phantom of a slit chamber has shown accuracy in the range of few mm on the beam range on proton beam. The use of charged particles seems to be promising only if applied to carbon ion treatment of head–neck tumors mainly due to the re-absorbing inside the patient of the charged secondary produced by the beam.

A comparison among the three proposed techniques (PET, PG and charged fragments) is not trivial. One reason is that many of the proposed detectors are in a research and development stage with not yet firmly established performances. Another cause of uncertainty in the field is the yet not completely reliable description of the nuclear interactions in the MC software used for the detector design. This second issues is rapidly evolving, both for the increasing amount of data gathered on the secondary emission produced by the beam and to a impressive work of modeling from the MC developers. An example of the achieved results is shown in Refs. 5 and 51 for PET and PG.

Finally, the relative performance of the three techniques change with the tumor size and position and the absolute dose release. In particular the prompt signal seems well suited to be exploited in case of a hypofractionated treatment, where the dose release in a single irradiation session, and the related secondary yields, can be almost one order of magnitude larger than the standard session.

A possible future solution is the use of integrated systems that exploit simultaneously two or more secondary signals. A first example of this method is the INSIDE-monitor system where two planar PET heads made of pixellated LYSO crystals are coupled to a large area tracker made of orthogonal layers of scintillating fibers. The PET subsystem has TOF and DAQ capabilities that allow for in-beam data taking while the tracker is focused on the detection of charged secondaries emitted at large angle (60°–90°) with respect to the beam. The goal resolution of this integrated device is of the order of few mm on the range of a single pencil beam of a 2 Gy treatment section, both on carbon or proton beams.

References

1. A.-C. Knopf and A. Lomax, *Phys. Med. Biol.* **58**, R131 (2013).
2. A. Fasso *et al.*, arXiv:hep-ph/0306267.
3. S. Agostinelli *et al.*, *Nucl. Instrum. Methods Phys. Res. A*: *Accel. Spectrom. Detect. Assoc. Equip.* **506**, 250 (2003).
4. G. W. Bennett *et al.*, *Science* **200**, 1151 (1978).
5. A. C. Kraan *et al.*, *Phys. Med.* **30**, 559 (2014).
6. M. Priegnitz *et al.*, *Phys. Med. Biol.* **53**, 4443 (2008).
7. K. Parodi, W. Enghardt and T. Haberer, *Phys. Med. Biol.* **47**, 21 (2002).
8. C. Agodi, arXiv:1202.1676.
9. M. Aiello *et al.*, A dose determination procedure by PET monitoring in proton therapy, in *2011 IEEE Nuclear Science Symp. Conf. Record* (IEEE, 2011), pp. 3534–3538.
10. I. Pshenichnov, I. Mishustin and W. Greiner, *Phys. Med. Biol.* **51**, 6099 (2006).
11. A. Knopf *et al.*, *Phys. Med. Biol.* **54**, 4477 (2009).
12. J. Bauer *et al.*, *Radiother. Oncol.* **107**, 218 (2013).
13. F. Fiedler *et al.*, *Acta Oncol.* (*Sweden*) **47**, 1077 (2008).
14. T. Nishio *et al.*, *Int. J. Radiat. Oncl. Biol. Phys.* **76**, 277 (2010).
15. X. Zhu *et al.*, *Phys. Med. Biol.* **56**, 4041 (2011).
16. W. Enghardt *et al.*, *Strahlenther. Onkol.* **175**, 33 (1999).
17. W. Enghardt *et al.*, *Nucl. Phys. A* **654**, 1047c (1999).
18. W. Enghardt *et al.*, *Radiother. Oncol.* **73** (Suppl. 2), S96 (2004).
19. K. Parodi *et al.*, *Nucl. Instrum. Methods Phys. Res. A*: *Accel. Spectrom. Detect. Assoc. Equip.* **545**, 446 (2005).
20. D. Unholtz *et al.*, Post-therapeutical $\beta+$ activity measurements in comparison to simulations towards *in-vivo* verification of ion beam therapy, in *2011 IEEE Nuclear Science Symp. Conf. Record* (IEEE, 2011), pp. 2273–2276.
21. F. Attanasi *et al.*, *Phys. Med. Biol.* **54**, N29 (2009).
22. S. Vecchio *et al.*, *IEEE Trans. Nucl. Sci.* **56**, 51 (2009).
23. G. Sportelli *et al.*, *Phys. Med. Biol.* **59**, 43 (2014).
24. J. R. Styczynski, Assessment of the use of prompt gamma emission for proton therapy range verification (2009), http://hdl.handle.net/1721.1/54468.
25. F. Le Foulher *et al.*, *IEEE Trans. Nucl. Sci.* **57**, 2768 (2010).
26. K. S. Seo, H. C. Kim and J. W. Kim, *J. Korean Phys. Soc.* **48**, 855 (2006).
27. C.-H. Min *et al.*, *Appl. Phys. Lett.* **89**, 183517 (2006).
28. C. H. Kim *et al.*, *J. Korean Phys. Soc.* **50**, 1510 (2007).
29. J. C. Polf *et al.*, *Phys. Med. Biol.* **54**, 731 (2009).
30. J. C. Polf *et al.*, *Phys. Med. Biol.* **54**, N519 (2009).
31. J. C. Polf *et al.*, *Phys. Med. Biol.* **58**, 5821 (2013).

32. E. Testa *et al.*, *Appl. Phys. Lett.* **93**, (2008).
33. E. Testa *et al.*, *Nucl. Instrum. Methods Phys. Res. B*: *Beam Interact. Mater. At.* **267**, 993 (2009).
34. C. Agodi *et al.*, *J. Instrum.* **7**, P03001 (2012).
35. F. Bellini *et al.*, *Nucl. Instrum. Methods Phys. Res. A*: *Accel. Spectrom. Detect. Assoc. Equip.* **745**, 114 (2014).
36. J. Smeets *et al.*, *Phys. Med. Biol.* **57**, 3371 (2012).
37. V. Bom, L. Joulaeizadeh and F. Beekman, *Phys. Med. Biol.* **57**, 297 (2012).
38. S. W. Peterson, D. Robertson and J. Polf, *Phys. Med. Biol.* **55**, 6841 (2010).
39. D. Robertson *et al.*, *Phys. Med. Biol.* **56**, 3047 (2011).
40. S. Kurosawa *et al.*, *Current App. Phys.* **12**, 364 (2012).
41. E. Haettner *et al.*, *Phys. Med. Biol.* **58**, 8265 (2013).
42. K. Gwosch *et al.*, *Phys. Med. Biol.* **58**, 3755 (2013).
43. R. Pleskac *et al.*, *Nucl. Instrum. Methods Phys. Res. A*: *Accel. Spectrom. Detect. Assoc. Equip.* **678**, 130 (2012).
44. C. Agodi *et al.*, *J. Phys. Conf. Ser.* **420**, 012061 (2013).
45. N. Matsufuji *et al.*, *Phys. Med. Biol.* **50**, 3393 (2005).
46. E. Haettner, H. Iwase and D. Schardt, *Radiat. Prot. Dosim.* **122**, 485 (2006).
47. K. Gunzert-Marx, H. Iwase, D. Schardt and R. S. Simon, *New J. Phys.* **10**, 075003 (2008).
48. B. Braunn *et al.*, *Nucl. Instrum. Methods Phys. Res. B*: *Beam Interact. Mater. At.* **269**, 2676 (2011).
49. P. Henriquet *et al.*, *Phys. Med. Biol.* **57**, 4655 (2012).
50. L. Piersanti *et al.*, *Phys. Med. Biol.* **59**, 1857 (2014).
51. C. Robert *et al.*, *Phys. Med. Biol.* **58**, 2879 (2013).